A Framework for Rapid Diagnosis of Critical Faults in Unmanned Aerial Vehicles

Søren Hansen * **Mogens Blanke** *,*** **Jens Adrian** **

* *Technical University of Denmark, Department of Electrical Engineering, Automation and Control Group, Elektrovej B. 326, DK-2800 Lyngby. Denmark.*
** *Danish Forces Joint UAV Team, Naval Weapons School, Gnibenvej 55, DK-4583 Sjællands Odde. Denmark.*
*** *AMOS Centre of Excellence, Norwegian University of Science and Technology, NTNU, NO-7491 Trondheim, Norway.*
(E-mail: sh@elektro.dtu.dk, mb@elektro.dtu.dk)

Abstract: Unmanned Aerial Vehicles (UAVs) need a large degree of tolerance towards faults. If not diagnosed and handled in time, many types of faults have catastrophic consequences, if they occur during flight. Prognosis of faults is also valuable and so is the ability to distinguish the severity of the different faults in terms of both consequences and the frequency with which they appear. In this paper flight data from a fleet of UAVs is analysed with respect to certain faults and their frequency of appearance. Data is taken from a group of UAV's of the same type but with small differences in weight and handling due to different types of payloads and engines used. Categories of critical faults, that could and have caused UAV crashes are analysed and requirements to diagnosis are formulated. Faults in air system sensors and in control surfaces are given special attention. In a stochastic framework, and based on a large number of data logged during flights, diagnostic methods are employed to diagnose faults and the performance of these fault detectors are evaluated against flight data. The paper demonstrates a significant potential for reducing the risk of unplanned loss of remotely piloted vehicles used by the Danish Navy for target practice.

1. INTRODUCTION

Fault Diagnosis (FD) and Fault Tolerant Control (FTC) are techniques that can strengthen safety-critical systems, such as controllers for Unmanned Aerial vehicles (UAV), and make them more reliable. A more reliable control system will of course produce a more beneficial and useful end product, in this case for the entire Unmanned Aircraft System (UAS). It is therefore important to include aspects of fault diagnosis when designing a system. However in some cases, for various reasons, this is not done. This paper explores the possibilities to add on a diagnosis framework to an existing UAS, where the aircraft do not have a build in FD/FTC systems. The system is tested against a couple of known faults that has occurred on these types of aircraft and where the existing controller reacted undesirable, but where information about the imminent fault was available in sensor data.

A lot of research has been done to improve the overall safety and reliability of UAV's. Generic treatment of the subject is done in Edwards et al. (2010) and Zolghadri et al. (2013) which highlights some of the major advances done within in the recent years. A full treatment of how to accommodate to faults affecting the control of a UAS was shown in Ducard and Geering (2008) and Ducard (2009) where manoeuvrability was the main focus area.

Treatment of specific faults related to aircraft has been extensively studied and partly reported in the literature. For the case of control surface loss, estimation of the reduced flight envelope and active FD was dealt with by Bateman et al. (2011). In Henry et al. (2012), methods using linear parameter varying methods were shown to be efficient for this problem. Research on the airspeed sensor related issues have been treated in Samy et al. (2011) and Wheeler et al. (2011) who analysed performance of linear time-invariant fault detection methods applied on parallel airspeed sensors.

This overview paper draws upon results from airspeed sensor system diagnosis (initial results in Hansen et al. (2010) and a detailed scrutiny in Hansen and Blanke (2014)) and diagnosis of control surface defects (with different approaches presented in Hansen and Blanke (2012), Hansen and Blanke (2013) and Blanke and Hansen (2013)). The paper is organised in four sections. Following this brief introduction a description is provided of the diagnosis system and the system it is made for. After this description of the types of faults considered within this system which precedes an example of the diagnosis system and a conclusion.

2. BACKGROUND AND CONTEXT

The Danish Navy uses remotely piloted drones for target practice and other tasks. These aircraft are constructed with aim at low complexity and low cost. They lack redundancy in sensors and actuators and the build in

Preprint submitted to 19th IFAC World Congress. Received November 19, 2013.

avionics is non-redundant as well. The type of drone dealt with in this paper lands by parachute, hence the remedial action to critical faults will be an abortion of mission and release of the parachute. Graceful degradation is possible to a certain extent but need to be activated via telemetry: operator commands can reconfigure the onboard autopilot between a few predetermined modes and gains could be changed. However, time to react to critical faults is rather short, typically in the order seconds to minutes, so very clear diagnostic messages and decision support need be provided to an operator if he shall have time to react in time.

Systems that are constructed with fault tolerance in mind already from the design stage, would have a system and software architecture that enable diagnosis and fault accommodation. The means to do so are well known but have emerged only slowly in aerospace applications Bak et al. (1996), Goupil (2010). With an avionics operator (AVO) in the loop, diagnosis need be timely and the ratio between detection and false alarm probability must be very high. Otherwise, the diagnostic system will soon loose credibility by the AVO's rendering the decision support useless.

The aim for the research collaboration described in this paper was hence,

- Make early warning possible from telemetry data
- Make detection and false alarm probabilities essential design parameters
- Use mainly data driven diagnosis as detailed modelling may not be an option
- Ensure robustness to parameter changes due to loading etc

The starting point for this diagnosis framework is a low-complexity UAV used for target practice which has the basic sensor suit consisting of IMU (Inertial Measurement Unit), airspeed sensor, height sensor and a GPS receiver. An onboard autopilot controls the aircraft to follow a route of waypoints send to it from a base station. The route can be changed online however the aircraft must at all time be within range of the base stations radio transmitter. More details about the UAS can be found in Meggitt Defence Systems Ltd. (2008).

3. DIAGNOSIS SETUP DESCRIPTION

Without adding any new hardware or modify the existing control system, an attempt to diagnose certain critical faults using a low-complexity aircraft model and the available telemetry data.

The general approach is shown in Fig. 1. Given the commands it is possible to calculate the expected behaviour of aircraft. By comparing this to the sensor values returned in the aircraft telemetry it is possible generate residual signals. Small variations in these residual signals can be used to tune the model parameters to better describe the specific aircraft and the influences of surrounding factors such as wind. A large variation on the residuals indicate a fault. The ability to distinguish variations due to disturbances form variations due to faults is critical for this setup. The Generalised Likelihood Ratio Test (GLRT) has been used for change detection, with good results. The

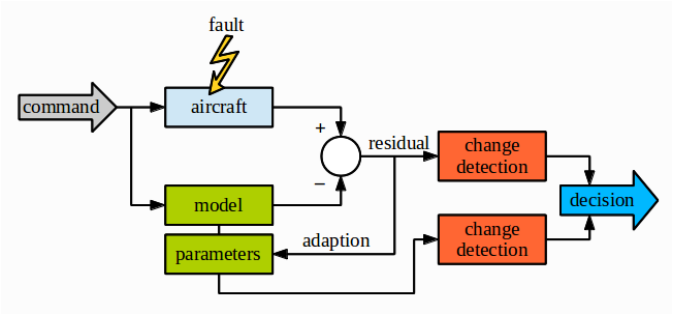

Fig. 1. Block diagram of the diagnosis setup.

GLRT is used to distinguish between the following two hypothesis about signal x at sample n.

$$\begin{aligned} \mathcal{H}_0 &: x_n = w_n \\ \mathcal{H}_1 &: x_n = A + w_n. \end{aligned} \tag{1}$$

The $\mathcal{H}_0$ hypothesis is the nominal case where the expected noise w is present. In the alternative $\mathcal{H}_1$ hypothesis the signal has been offset by a mean around 0 by some value A. If the difference between observations and the model are statistically significant within a desired false alarm probability (P_F) and detection probability P_D a fault hypothesis is confirmed. GLRT detectors are derived according to the observed distribution of residuals.

From Fig. 1 it is also realised that an effect of a fault will be present on the model parameters as a result of the adaptation feedback from the residual. Changes on the model parameters are therefore also monitored by GLRT. A significant increase in the performance of the diagnosis system was achieved by combining both change detector outputs, utilising the joint distribution of test statistic for residuals and parameters, see Blanke and Hansen (2013) for details. It is noted that the parameter adaptation of the residual generator is halted when residual's test statistic change. Otherwise faults would be masked and change detection using the strong detectability assumption of the model 1 could not be applied on residuals.

To distinguish between the hypotheses (1) the GLRT expresses a ratio between the two maximum likelihood estimates over a data window of size M given the residual $\boldsymbol{x(i)}$ and subject to the hypothesis 1,

$$S_j^k(\boldsymbol{x}, A) = ln \sum_{i=k-M}^{k} \frac{p\left(\boldsymbol{x(i)}; \mathcal{H}_1\right)}{p\left(\boldsymbol{x(i)}; \mathcal{H}_0\right)} \tag{2}$$

The well-known GLRT test statics $g(k)$ for the model 1 is obtained for a Gaussian, IID signal $x(i)$ as

$$g(k) = \max_{k-M \le j \le k} \max_{A} S_j^k(\boldsymbol{x(i)}, A) \tag{3}$$

where j is the hypothetical instant when the change occurs. The decision $\mathcal{H}_1$ is taken if $g(k) > \gamma$ where A and the change instant are estimated by the GLRT. The threshold value γ is usually fixed or time-varying (adaptive), as used by Verdier and Vila (2008), but an obstacle is that theoretical calculation of γ requires the distribution of residuals to be known and the residual itself to be IID. An obstacle to residual evaluation is that residuals observed from numerous UAV flights show heavily correlation. The setup employed in this paper is therefore to estimate a

threshold from data: the distribution of test statistic is estimated and a threshold is calculated based on a required P_F. This approach was introduced in Blanke et al. (2012) and further explored in Galeazzi et al. (2013)).

Figure 2 shows the cumulative distribution function (CDF) for the test statistic ($g(k)$) of residuals for normal flights ($\mathcal{H}_0$. The dotted line in the probability plot is the estimated CDF for the distribution. A false alarm probability $P_F = 0.0005$ is obtained by selecting $\gamma = 50$ on the abscissa axis that corresponds to $1 - P_F = 0.9995$ on the ordinate axis. The test statistic is denoted T_L in the title fields of the plots.

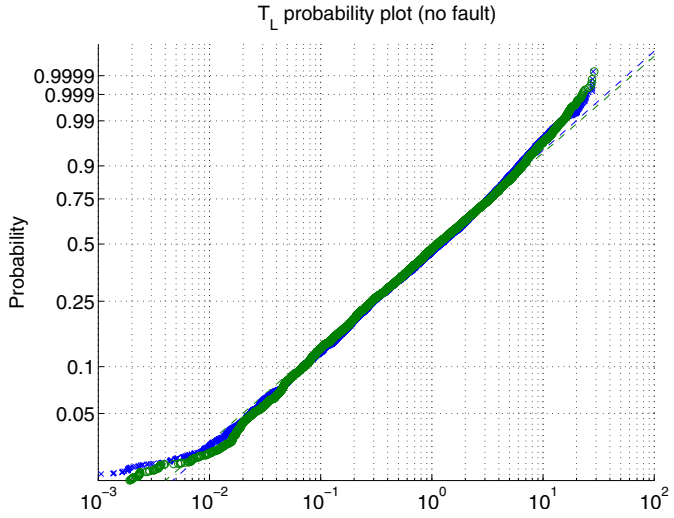

Fig. 2. Probability plot of the change detectors output when no fault is present. Results from several flights.

Figure 3 shows the CDF of data during $\mathcal{H}_1$ for two different control surface faults. Case I is a low severity mechanical slip of an aileron actuator where the AVO should be warned about the fault but mission could be continued, however at higher risk. The low detection probability $P_F = 0.5$ would be an issue with this fault and supplementary information from parameter estimation could be beneficial. Case II is a high severity event giving loss of control of an aileron where early detection is essential to allow the AVO sufficient time to react to the event.

4. FAULT CATEGORIES INVESTIGATED

Within this framework, mainly two categories of faults has been investigated since data logs from several events of these types were available for analysis. The faults are: a) *airspeed system defects*, b) *control surface actuator or fin detects*. The defects are subdivided according to their severity: level L has low severity, aircraft flight envelope is not affected during normal manoeuvres; level H has high severity, aircraft flight envelope is affected during normal manoeuvres.

A summary of flight records available without any faults and with either of these types of defects are shown in Table 1. Both fault types has a course which makes them well suited for this kind of diagnosis in that they are visible in the telemetry data some time before aircraft control is lost, in case of severity level H, and for the remaining

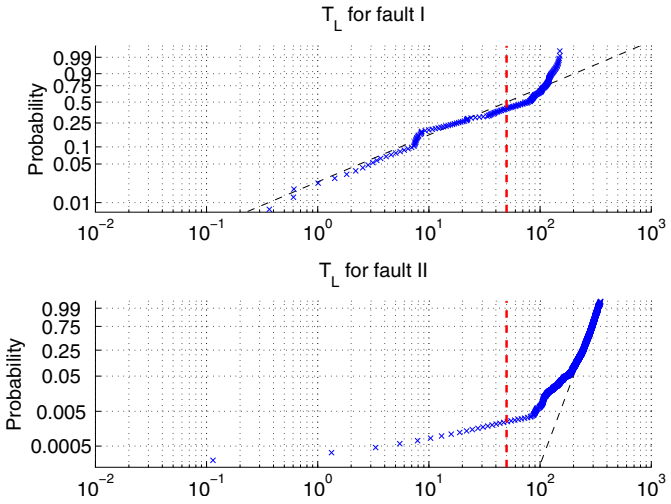

Fig. 3. Probability plot of the change detectors output for different faults.

Table 1. Flight time records in minutes under not normal conditions and all analysed flights

	time with fault	time span analysed
airspeed sensor	3.9	1500
control surface (sev. L)	158.9	1250
control surface (sev. H)	0.7	1250

duration of flight in case of severity level L. This means that a certain reaction time is available for the AVO to react to a timely warning about a defect diagnosed.

It is important to note that one cannot draw any conclusions on aircraft reliability based on the numbers in Table 1. This only shows the amount of data analysed during designs of the different parts of the diagnosis system. The amount of flight time with a fault is also limited for the level H faults, since these always leads to a crash fairly quickly after occurrence.

4.1 Airspeed System Defect

In order to measure the airspeed a pitot static system is often employed on aircraft. By measuring the pressure difference between two ports mounted on the body of the aircraft it is possible to measure the airspeed. This is an important measure since it enables the control system to keep the aircraft within its specified velocities and avoid stalls. The pitot static system used is very sensitive to clogging of the ventilation ports. Especially moist or dew on the aircraft tends to freeze up in higher altitudes and can clog the ports.

Fig. 4 shows data from an incident with icing of a pitot tube. The aircraft ground speed estimated by the GPS is plotted together with the airspeed indicate by the pitot static system. At approximately $t = 2140$ s the fault begins to be visible as a high increase in the ground speed compared to airspeed. The increase in speed is the autopilot responding to the decrease in measured airspeed as a result of the fault.

Using the measurements often available on this type of aircraft, namely, the airspeed measurement v_{pitot}, velocity measured by GPS and compensated for wind $v_{gps2air}$, and

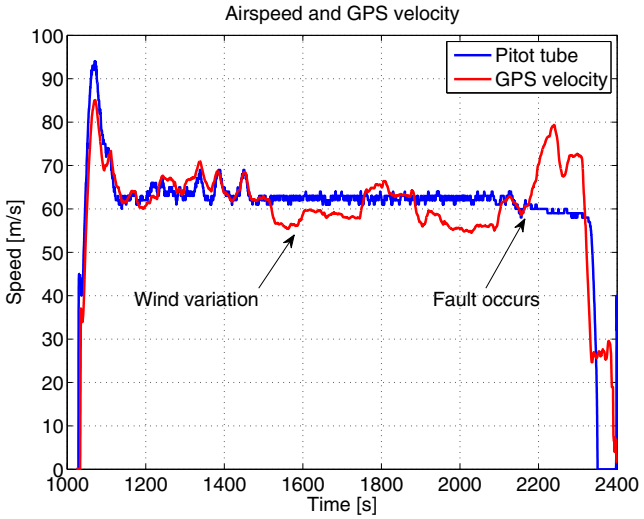

Fig. 4. Data from pitot tube and GPS velocity shown for a case where the pitot tube clogs.

the expected velocity v_{thrust} obtained at a known engine shaft speed, it is possible to obtain a set of residuals describing the differences between these measurements. This gives rise to three residuals described by their parity relations shown in Table 2. In the table a "1" indicate that

Table 2. Parity relations.

Residual	v_{pitot}	$v_{gps2air}$	v_{thrust}
R_1	1	1	0
R_2	1	0	1
R_3	0	1	1

the current residual is depending on this variable. This means that a fault occurring on v_{pitot} will affect residual R_1 and R_2, but not R_3. This scheme will however not work if faults involving more than one of the parameters occurs at the same time.

The actual generation of the different speed estimates is obtained by different types of estimates. The main problem in using the GPS velocity is to transform this to airspeed. An estimate of the wind field is needed to make the connection between ground- and airspeed.

To obtain this connection a simplified 2D perspective on the velocities is taken. The aircraft velocity relative to air $\boldsymbol{v}_{rel}$ is related to the ground speed vector $\boldsymbol{v}_g$ with this vector sum: $\boldsymbol{v}_g = \boldsymbol{v}_{rel} + \boldsymbol{v}_w$. The wind velocity vector, $\boldsymbol{v}_w$ is defined such that it points in the direction the wind blow. The size of the airspeed can then be formulated using the standard cosine rule for triangles

$$v_{rel}^2 = v_w^2 + v_g^2 - 2v_g v_w \cos(\psi_w - \psi_g), \tag{4}$$

where the vectors are put into polar form. In this, ψ_w, is the wind angle and the heading of the aircraft is denoted ψ_g.

The airspeed measurement given by the pitot tube is offset by the aircraft angle of attack α and side slip β, in relation to v_{rel}. Since measurements of α and β are not available the following simplified conversion is used:

$$v_{pitot} = \cos(\alpha)\cos(\beta)v_{rel} \simeq a v_{rel} \tag{5}$$

An Extended Kalman Filter (EKF) is now used to estimate $[v_w, \psi_w, a]^{\mathrm{T}}$. These are modelled as random walk processes. By using the EKF estimates and combining (4) and (5) it is possible to generate a residual honouring the first row in Table 2.

$$R_1 = v_{pitot} - \hat{a}\sqrt{\hat{v}_w^2 + v_{gps}^2 - 2v_{gps}\hat{v}_w \cos(\hat{\psi}_w - \psi_{gps})} \tag{6}$$

The thrust based velocity v_{thrust} is generated using a model of the engine and propellers delivered thrust at certain throttle settings. The longitudinal dynamics can in general be described by:

$$m\dot{v}_{pitot} = m(rv - qw) + F_{Ax} - mg\sin(\theta) + F_T \tag{7}$$

with $[p, q, r]^{\mathrm{T}}$ being the angular rates of the aircraft, θ the pitch angle, m the mass, F_T the thrust force and F_{Ax} the aerodynamic force in this axis. This is approximated by

$$F_{Ax} = \tfrac{1}{2}\varrho S v_{pitot}^2 \Theta_{uu} = mF_1(v_{pitot}, t) \tag{8}$$

Using an observer v_{pitot} can be estimated using the dynamic equation and thereby the second residual of Table 2 is formed.

$$R_2 = v_{pitot} + \left(\int g\sin(\theta) - \frac{T_{nn}n^2 + T_{nu}n\hat{v}_{pitot}}{m} - F_1(\hat{v}_{pitot}, t)\hat{\Theta}_{uu}dt\right) - L(v_{pitot} - \hat{v}_{pitot}). \tag{9}$$

With n being the propeller angular velocity, T_{nn} and T_{nu} is thrust coefficient of the propeller, and L is the observer gain.

Following the voting scheme described in Table 2 the third residual is the difference between the two estimates of airspeed. Since both $v_{gps2air}$ and v_{thrust} relies on the airspeed measurement in their estimation procedures, it is impossible achieve independence of v_{pitot}. However, since the purpose of R_3 is to ensure isolability of the airspeed measurement fault, its value is only required when R_1 and/or R_2 indicate an alarm. With

$$R_3 = v_{gps2air} - v_{thrust} \tag{10}$$

and setting adaptation on hold when a fault is detected, R_3 can be used for isolation. If an airspeed fault is detected, v_{pitot} can not re-enter in calculations that estimate $v_{gps2air}$ and v_{thrust}. These estimates will therefore after a while become increasingly uncertain, which in turns affects R_3. However, as long as R_3's value is reliable up to and shortly after detection, it serves the purpose.

4.2 Control Surface or Actuator Defect

One of the most critical faults that can happen to an aircraft is partly or totally loss of one of the control surfaces. This reduces manoeuvrability of the aircraft significantly and will in most cases lead to a crash. This is a defect of severity level 3. Less critical faults include misalignment of the actuator to fin linkage and will mainly affect steady state trim and also the available range of control surface deflection, the latter due to mechanical limits.

An example of a incident of this type is given in Fig. 5. The figure shown the selected telemetry data for the aircraft up to and just after loss of an aileron. Just before

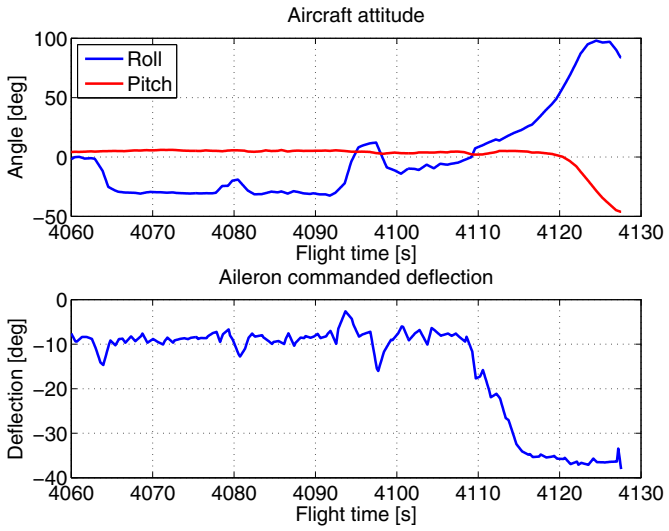

Fig. 5. Top: Roll and pitch signals. Bottom: Command signal to ailerons. An incident where control of an aileron is lost during flight.

$t = 4110$ s the aircraft starts rolling right, even though the commanded signal is for a left roll. From this point on there is no relation between the commanded signal and the aircraft's manoeuvres. The aircraft crashes shortly after and the subsequent investigation of the crash determined that control of an aileron was lost in flight.

A system to diagnose this type of fault can be created using the dynamic models of the aircraft. Aircraft mathematical modelling requires a 6 degree of freedom model, where both dynamic and kinematic equations of motion are needed to characterise the aircraft, see eg. Stevens and Lewis (2003). Utilising this model implies detailed knowledge about the aerodynamic coefficients and this information is not always available for the cheaper UAV's. For control surface fault diagnosis the important feature is the relationship between surface deflection and angular rates of the aircraft. In this paper an adaptive model of this relationship is employed. The following three relations for roll rate (p), pitch rate (q) and yaw rate (r), calculated at sample k, is related to the aileron deflection δ_a and elevator deflection δ_e.

$$p[k] = a_{pa}\delta_a[k] + b_{pa} \tag{11}$$
$$q[k] = a_{qe}\delta_e[k] + b_{qe} \tag{12}$$
$$r[k] = a_{ra}\delta_a[k] + b_{ra}r[k-1] + c_{ra} \tag{13}$$

where b_{pa}, b_{qe} and c_{ra} are bias terms and a_{pa}, a_{qe} and a_{ra} are gain factors. Equation (13) includes the integrating effect between the aileron and yaw rate in the b_{ra} term. This approach separates the lateral and longitudinal states since the aileron is only related to roll and yaw and the elevator is related to pitch.

Each of the parameters in equations (11) - (13) must be determined to fit the aircraft response to get the best result of the diagnosis as possible. From the block diagram of Fig. 1 it is seen that the parameters are adapted during flight such that small deviations from aircraft to aircraft are removed. The equations are on a form of an ARX function and hence a Recursive Least Squares (RLS) filter, as the following, can be used to estimate the parameters.

$$\varepsilon[k] = y[k] - \boldsymbol{\varphi}[k]^{\mathrm{T}}\hat{\boldsymbol{\Theta}}[k-1] \tag{14}$$
$$P[k] = \left(\lambda_f P[k-1]^{-1} + \boldsymbol{\varphi}[k]\boldsymbol{\varphi}[k]^{\mathrm{T}}\right)^{-1} \tag{15}$$
$$\hat{\boldsymbol{\Theta}}[k] = \hat{\boldsymbol{\Theta}}[k-1] + P[k]\boldsymbol{\varphi}[k]\varepsilon[k]. \tag{16}$$

In this, λ_f is the forgetting factor and $P[k]$ is the covariance. The initial value of $P[k]$ can be determined from some average of test flights: running the estimator for data from steady wings-level flight without faults would give an a-priori value of $P[k]$. The forgetting factor is tunable and this is one of the parameters to be considered when combining parameter identification with residual evaluation for diagnosis. Control surface defects will give rise to rapid change in the input/output signals and hence in the prediction error (14) and subsequently appear as a parameter adaptation to the faulty case.

5. DIAGNOSIS EXAMPLE

In this section a short example of the diagnosis system is given. The fault is one of the servos controlling a aileron flap slipping in its teeth. In Fig. 6 data from two of the residuals is shown. In the figure a shaded area is put in

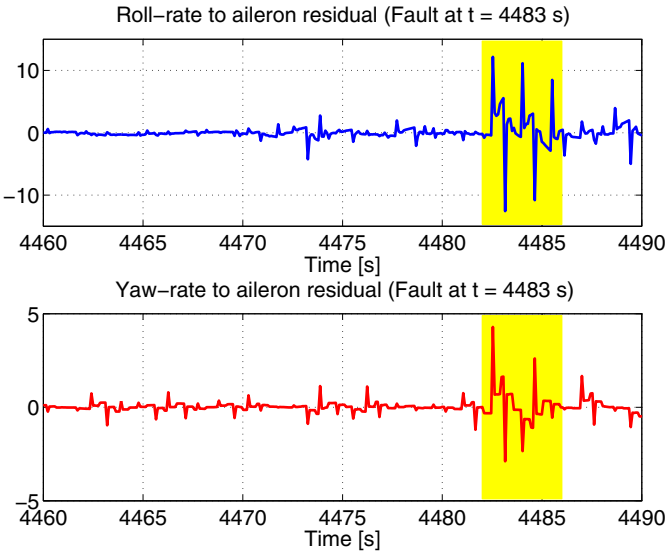

Fig. 6. Residuals for a servo fault. The fault occurs in the shaded area.

where the fault occurs. The fault is not critical for the continues flight and therefore of severity L according to Table 1. The detection of the fault is delayed 20 s from its occurrence due to effects of the windowing in the change detectors.

In Fig. 8 a probability plot of the change detector output is shown. The vertical black line indicates the detector threshold of 50 and therefore values above this raises an alarms. Data points for the entire shaded area of Fig. 6 are plotted. Around 10% of the data is above the threshold level.

Fig. 7 shows probability plots for change detector outputs for three different flights with no faults occurring. Com-

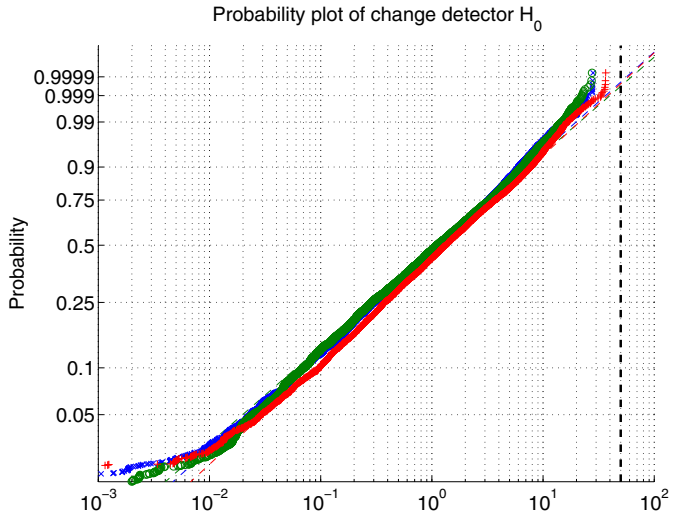

Fig. 7. Probability plot of three flights under $\mathcal{H}_0$ with detection threshold.

paring to Fig. 8 shows that all signals stay well below the threshold.

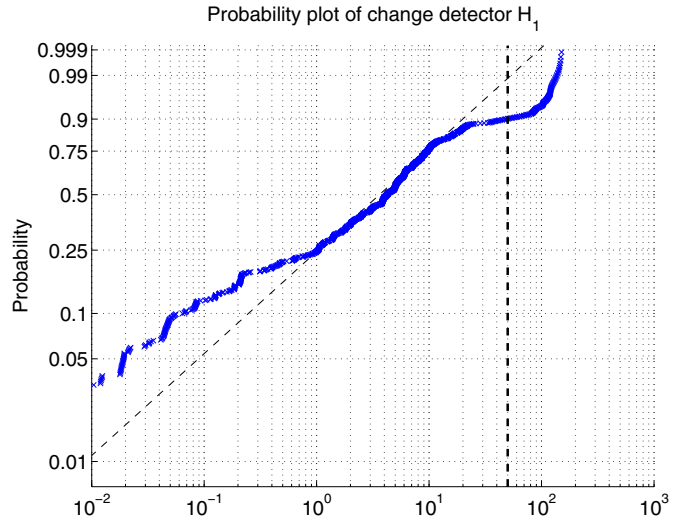

Fig. 8. Probability plot of three flights under $\mathcal{H}_1$ with detection threshold.

In Fig. 9 a scatter diagram of the change detector output and two parameters of (13) is shown. This shows little change in parameter value for the faulty case whereas the change detector has a large change of value when the fault occurs. This shows that for this specific fault the best detection can be obtained using the residual values.

6. CONCLUSION

This paper has given an overview of a fault diagnosis system designed to diagnose two high severity types of faults for a UAV. The diagnosis approach assumed that only basic system knowledge and standard UAV sensors where available and employed self-tuning methods to generate models for diagnosis. Diagnosis was designed to work on telemetry data from the aircraft. Examples of the capabilities of the diagnostic was demonstrated. High severity faults were detected rapidly and, in the cases investigated, timely enough to avoid a failure. Low severity events were

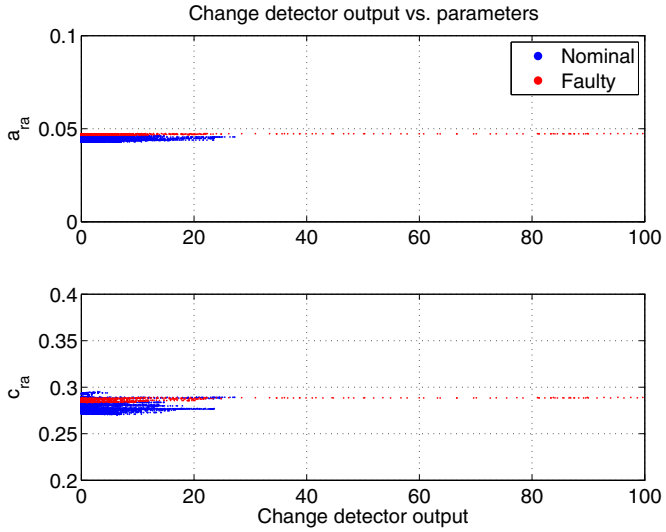

Fig. 9. Scatter plot of the residuals change detector output and the model parameters.

diagnosed with low probability of false alarm but further improvement are envisaged to be obtainable from exploitation of the joint probability between parameter estimates and residual test statistic.

ACKNOWLEDGEMENTS

The support from the Danish Forces Joint UAV Team in conducting experiments is greatly appreciated. The authors also wish to acknowledge the collaboration with Meggitt Defence Systems, UK, for providing access to telemetry data protocols for their systems.

REFERENCES

Bak, T., Wisniewski, R., and Blanke, M. (1996). Autonomous attitude determination and control system for the oersted satellite. In *Proc. 1996 IEEE Aerospace Applications Conference*.

Bateman, F., Noura, H., and Ouladsine, M. (2011). Fault diagnosis and fault-tolerant control strategy for the aerosonde uav. *IEEE Trans. on Aerospace and Electronic Systems*, 47 (3), 2119–2137.

Blanke, M., Fang, S., Galeazzi, R., and Leira, B.J. (2012). Statistical change detection for diagnosis of buoyancy element defects on moored floating vessels. In *Proc. IFAC SAFEPROCESS*, 462–467.

Blanke, M. and Hansen, S. (2013). Towards self-tuning residual generators for uav control surface fault diagnosis. In *Proc. 2nd International Conference on Control and Fault-Tolerant Systems*, 37–42.

Ducard, G. and Geering, H.P. (2008). Efficient nonlinear actuator fault detection and isolation system for unmanned aerial vehicles. *Journal of Guidance, Control, and Dynamics*, 31 (1), 225–237. doi:10.2514/1.31693.

Ducard, G.J.J. (2009). *Fault-tolerant Flight Control and Guidance Systems*. Springer Verlag.

Edwards, C., Lombaerts, T.J.J., and Smaili, M.H. (eds.) (2010). *Fault Tolerant Flight Control: A Benchmark Challenge*. Springer.

Galeazzi, R., Blanke, M., and Poulsen, N.K. (2013). Early detection of parametric roll resonance on container

ships. *IEEE Transactions on Control Systems Technology*, 21(2), 489–503. doi:10.1109/TCST.2012.2189399.

Goupil, P. (2010). Oscillatory failure case detection in the a380 electrical flight control system by analytical redundancy. *Control Engineering Practice*, 18, 1110 – 1119.

Hansen, S. and Blanke, M. (2012). In-flight fault diagnosis for autonomous aircraft via low-rate telemetry channel. In *IFAC International Symposuim on Fault Detection, Supervision and Safety for Technical Processes*.

Hansen, S. and Blanke, M. (2013). Control surface fault diagnosis with specified detection probability - real event experiences. In *2013 International Conference on Unmanned Aircraft Systems*.

Hansen, S. and Blanke, M. (2014). Diagnosis of airspeed measurement faults for unmanned aerial vehicles. *IEEE Trans. Aerospace and Electronic Systems*, 50 (1).

Hansen, S., Blanke, M., and Adrian, J. (2010). Diagnosis of uav pitot tube defects using statistical change detection. In *7th Symposium on Intelligent Autonomous Vehicles*.

Henry, D., Zolghadri, A., Cieslak, J., and Efimov, D.V. (2012). A lpv approach for early fault detection in aircraft control surfaces servo-loops. In *IFAC Proceedings IFAC SAFEPROCESS'2012*, 806 – 811. Mexico City. doi:10.3182/20120829-3-MX-2028.00047.

Meggitt Defence Systems Ltd. (2008). Banshee aerial target system. URL `http://www.meggittdefenceuk.com/PDF/Banshee aerial target system.pdf`.

Samy, I., Postlethwaite, I., and Gu, D.W. (2011). Unmanned air vehicle air data estimation using a matrix of pressure sensors: a comparison of neural networks and look-up tables. *Journal of Aerospace Engineering*, 225 (7), 807–820.

Stevens, B.L. and Lewis, F.L. (2003). *Aircraft Control and Simulation*. John Wiley & Sons, 2nd edition.

Verdier, G. and Vila, N.H.A.J.P. (2008). Adaptive threshold computation for cusum-type procedures in change detection and isolation problerms. *Computational Statistics and Data Analysis*, 52, 4161–4174.

Wheeler, T.J., Seiler, P., Packard, A.K., and Balas, G.J. (2011). Performance analysis of fault detection systems based on analytically redundant linear time-invariant dynamics. In *Proc. 2011 American Control Conference (ACC 2011)*, 214–219.

Zolghadri, A., Henry, D., Cieslak, J., Efimov, D., and Goupil, P. (2013). *Fault Diagnosis and Fault-Tolerant Control and Guidance for Aerospace Vehicles - From Theory to Application*. Springer.